Kinetics of Propylene Polymerization by Hafnocene Diamide Catalyst

IL KIM, JIA-MIN ZHOU

Department of Chemical Engineering, The University of Ulsan, P.O. Box 18, Ulsan 680-749, Korea

Received 6 May 1998; accepted 23 November 1998

ABSTRACT: The kinetics of propylene polymerization initiated by *ansa*-metallocene diamide compound *rac*-(EBI)Hf(NMe_2)$_2$ (EBI = C_2H_4-(indenyl)$_2$, *rac*-**1**) were investigated. The *rac*-**1** compound could be directly utilized for catalyst formations without converting to a dihalide or dialkyl complex in the presence or absence of methylaluminoxane (MAO). The MAO-free system *rac*-**1**/AlR_3/[Ph_3C][$B(C_6F_5)_4$] (**2**) is much more effective than the *rac*-**1**/MAO catalyst. The activity of the *rac*-**1**/Al(*i*Bu)$_3$/**2** system is much higher than that of the *rac*-(EBI)$HfCl_2$/MAO or *rac*-(EBI)$ZrCl_2$/MAO catalyst, and almost same as that of the *rac*-(EBI)Zr(NMe_2)$_2$/Al(*i*Bu)$_3$/**2** catalyst under similar conditions. The alkylation of *rac*-**1** to *rac*-(EBI)HfR_2 by using AlR_3 needs more time than the corresponding zirconocene analogue. The activity increases by a factor of 7 by increasing the aging time from 1 min to more than 4 h. The activity of the *rac*-**1**/AlR_3/**2** catalyst is very sensitive to the type and concentration of AlR_3, and decreases in the order: Al(*i*Bu)$_2$H > Al(*i*Bu)$_3$ > $AlEt_3$ > $AlMe_3$. The catalyst keeps high activity in a narrow range of the [Al]/[Hf] ratio. In addition, the activity is influenced by the concentration of **2**, and as a result, the maximum activity is observed when **2**/*rac*-**1** = 0.7. The activity of the *rac*-**1**/AlR_3/**2** catalyst is also sensitive to the polymerization temperature. The activation energies for the initiation and overall reactions are calculated as 7.61 and 7.14 kcal/mol, respectively. The properties of polymer such as isotacticity (as [*mmmm*]), molecular weight (MW), molecular weight distribution (MWD), melting temperature (T_m), and crystallinity are similar level with those obtained with the *rac*-(EBI)$HfCl_2$/MAO system. The MW and isotacticity of the polymer produced by MAO-free system decreases monotonically as T_p increases, and MWD becomes narrow from 2.90 to 2.10 when T_p increases from 30 to 90°C because of the compositional homogeneity of the polymer produced at high T_p, which is demonstrated by fractionation of the polymer. Both MW and [*mmmm*] values of polymers decrease as aging time and anion concentration increase. © 2000 John Wiley & Sons, Inc. J Appl Polym Sci 75: 843–855, 2000

Key words: *ansa*-hafnocene diamide; kinetics; propylene polymerization; methylaluminoxane-free cocatalyst; properties of polypropylene

INTRODUCTION

The metallocene compounds of the group 4 metals have been very extensively developed as catalysts for olefin polymerization.[1] As a basic bridged metallocene, *rac*-(EBI)$ZrCl_2$ (EBI = C_2H_4-(indenyl)$_2$) has been reported to produce highly isotactic polypropylene (*i*PP) by coactivating with methylaluminoxane (MAO).[2] The *i*PP is characterized by a narrow molecular weight distribution (MWD) and a low molecular weight (MW).[3] It is already known that the MW of polymers can be

Correspondence to: I. Kim.
Contract grant sponsor: Korea Research Foundation.

Journal of Applied Polymer Science, Vol. 75, 843–855 (2000)
 CCC 0021-8995/00/060843-13

increased with using hafnium components.[4] By using the analogous hafnium catalyst system (*rac*-(EBI)$HfCl_2$/MAO), Ewen[5] was able to increase MW of polypropylene by a factor of 10. Unfortunately hafnium catalysts are much less active than their zirconium analogues.[1a,1m] For example, the activity of the *rac*-(EBI)$ZrCl_2$/MAO catalyst is higher than that of the *rac*-(EBI)$HfCl_2$/MAO catalyst by a factor of 10.[1m]

Current synthetic routes of *ansa*-metallocenes based on salt elimination reactions of MCl_X salts and bis-cyclopentadienyl dianion reagents are inefficient and require tedious separation and purification steps. Brintzinger and Collins prepared the prototypical *rac*-(EBI)$ZrCl_2$ by a reaction of $ZrCl_4$(THF) and (EBI)Li_2, and reported low, variable yield (30–50%).[6] Buchwald employed (EBI)K_2, and obtained *rac*-(EBI)$ZrCl_2$ in a 70% yield, with only a *rac/meso* ratio of 2/1.[7] In addition, current salt elimination syntheses of *rac*-(EBI)$HfCl_2$ are even less efficient than *rac*-(EBI)-$ZrCl_2$. The reaction of $HfCl_4$ and (EBI)Li_2 in THF affords *rac*-(EBI)$HfCl_2$ in an 11% yield,[5] and the use of high dilution and slow mixing of THF solutions of $HfCl_4$ and (EBI)K_2 increases the yield to only 37%.[7,8] The separation of the *rac* isomer from the *meso* isomer is always difficult.

Jordan recently reported an efficient synthesis method of *ansa*-metallocene $^{ch}Cp_2Zr(NR_2)_2$ ($^{ch}Cp_2Zr$ = chiral *ansa*-metallocene framework) via an amine elimination route.[9] They prepared *rac*-(EBI)$Zr(NMe_2)_2$ by the reaction of (EBI)H_2 and $Zr(NMe_2)_4$ with a 90% yield in a *rac/meso* ratio of 13/1.[9a] The reaction of (EBI)H_2 with $Hf(NMe_2)_4$ produced *rac*-(EBI)$Hf(NMe_2)_2$ (*rac*-**1**) in an 85% yield in a *rac/meso* ratio of 16/1.[9b] The separation of the *rac* isomer from the *meso* isomer is easy.

In this work, we have studied the kinetics of propylene polymerization by *rac*-**1** in the presence of MAO or alkyl aluminums (e.g., Al(iBu)$_3$, Al(iBu)$_2$H, $AlEt_3$, $AlMe_3$) combined with [Ph_3C][$B(C_6F_5)_4$] (**2**). The properties of the polymers are also characterized by various methods.

EXPERIMENTAL

Materials

All materials were handled with Schlenk or glovebox techniques under argon atmosphere. Toluene was distilled from sodium prior to use. Propylene of polymerization grade (SKC, Korea) was purified by passing it through columns of a Fisher RIDOX catalyst and molecular sieve 5A/13X. MAO (11.6 wt % Al) in toluene was purchased from Akzo Chemicals. Alkyl aluminums, Al(iBu)$_3$, Al(iBu)$_2$H, $AlEt_3$, and $AlMe_3$, were donated by Korea Petrochem. Co. and used without purification. The metallocene diamide, *rac*-**1**[9b], and the anionic compound, **2**[10], were synthesized according to literature procedures.

Propylene Polymerization

The polymerization was carried out in a 250-mL glass reactor. A Teflon magnetic stirring bar was used for the agitation. First, 80 mL toluene, the prescribed amount of AlR_3, and *rac*-**1** were introduced into the reactor sequentially in the glove box. After attaching the reactor to the polymerization setup, argon was pumped off and the reactor was then filled with propylene. After the temperature was stabilized at a desired point, the prescribed amount of **2** was injected into the reactor by a hypodermic syringe, and then the polymerization started. The reaction was quenched by introducing 150 mL ethanol containing HCl (5 vol %) into the reactor after 30 min of polymerization.

Characterization of Polypropylene

Thermal analysis of polymers was carried out by using Dupont differential scanning calorimeter (DSC, Model-900) at a 10°C/min heating rate under nitrogen atmosphere. The crystallinity is calculated from the heat of fusion, $(\Delta H_f/\Delta H_f^0) \times 100$, where ΔH_f is the heat of the fusion of the sample as determined from the DSC curve, and ΔH_f^0 is the fusion of a folded chain of isotactic polypropylene with a value of 208.3 J/g.[11] The intrinsic viscosity was measured in decalin at 135 ± 0.1°C using an Ubbelohde viscometer, and viscosity-average molecular weights were calculated as the following relationship:[12]

$$[\eta] = 1.0 \times 10^{-4} \overline{M_v}^{0.8} \quad (1)$$

Also tested were molecular weight and its distribution (M_w/M_n) by gel permeation chromatography (GPC) on a Waters 150-C at 135°C in 1,2-dichlorobenzene with a data processor,

equipped with polystyrene gel columns. ^{13}C-NMR spectra of polymers were recorded and measured at 120°C on a Varian Unity Plus 300 spectrometer operating at 75.5 MHz. Samples for ^{13}C-NMR spectra were prepared by dissolving 50 mg of polymer in 0.5 mL of benzene-d_6/1,2,4-trichlorobenzene-d_3 (1/5 v/v).

RESULTS AND DISCUSSION

In Situ Activation of *rac*-1

In the previous reports we showed that the $^{ch}Cp_2Zr(NR_2)_2$ compound is stoichiometrically alkylated by $AlMe_3$, while corresponding dichloride compound is only partly alkylated in the presence of excess $AlMe_3$:

$$^{ch}Cp_2Zr(NR_2)_2 + 4\ Al_2Me_6 \longrightarrow {}^{ch}Cp_2Zr(Me)_2 + 2\ Al_2Me_5(NR_2) \quad (2)$$

$$^{ch}Cp_2ZrCl_2 + Al_2Me_6\ (\text{excess}) \longrightarrow {}^{ch}Cp_2Zr(Me)Cl + Al_2Me_6\ (\text{excess}) \quad (3)$$

Addition of a noncoordinating anionic compound such as **2** or $[HNR_3][B(C_6F_5)_4]$ into the resulting mixture containing the $^{ch}Cp_2ZrMe_2$ compound affords *in situ* generation of cationic alkylzirconium species:

$$^{ch}Cp_2ZrMe_2 + [Ph_3C][B(C_6F_5)_4] \longrightarrow [{}^{ch}Cp_2ZrMe(\mu\text{-}Me)AlMe_2]^+ + [B(C_6F_5)_4]^- + Ph_3C(Me) \quad (4)$$

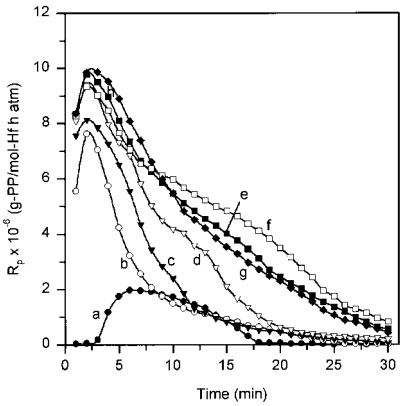

Figure 1 R_p vs. time plots initiated by *rac*-**1**/Al(iBu)$_3$/**2** with [Hf] = 31.3 μM, [Al]/[Hf]/**2** = 25/1/1, T_p = 50°C and P_{C3H6} = 1.3 atm with different aging times of (a) 1 min, (b) 0.5 h, (c) 1.5, (d) 2.5, (e) 4.0, (f) 7.0, (g) 12 h.

$$^{ch}Cp_2Zr(Me)_2 + [HNR_3][B(C_6F_5)_4] \longrightarrow [{}^{ch}Cp_2Zr(\mu\text{-}Me)_2AlMe_2]^+ + [B(C_6F_5)_4]^- + CH_4 + NR_3 \quad (5)$$

The alkylation usually happens immediately after introducing the aluminum compound into the mixture containing the $^{ch}Cp_2Zr(NR_2)_2$ compound. However, it seems that the present hafnocene, *rac*-**1**, needs a longer time to be alkylated by AlR_3. Figure 1 shows the propylene polymerizations obtained by changing the aging time. The aging time here is the contacting period of *rac*-**1** and Al(iBu)$_3$ before activation with **2**. The polymerization rate (R_p) is very low, with 1 min of aging time [Fig. 1(a)], and the lifetime (the time to reach zero polymerization rate) of the active sites is very short. With the increase of alkylating time from 1 min to 4 h, R_p increases continuously, and the lifetime of the active sites expands from less than 20 min to more than 30 min. Figure 2 plots the effect of aging time on the average rate of polymerization (R_p) and maximum rate ($R_{p,\max}$). The polymerization rates reach asymptotic values after the aging time of 4 h, indicating that at least 4 h is needed to alkylate *rac*-**1** to *rac*-(EBI)-Hf(iBu)$_2$ completely. If the alkylating time is not

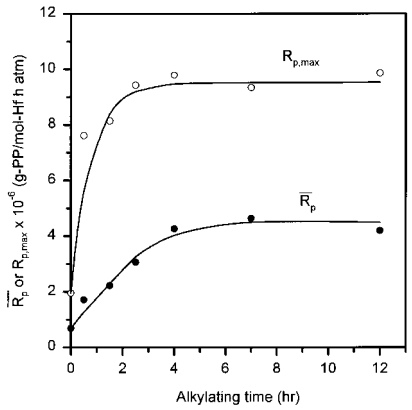

Figure 2 R_p and $R_{p,\max}$ vs. aging time plots. The polymerization conditions are as in Figure 1.

long enough, there exists nonalkylated, partially alkylated, and completely alkylated species, *rac*-**1**, *rac*-(EBI)Hf(*i*Bu)(NMe_2), and *rac*-(EBI)-Hf(iBu)$_2$, in the reaction medium. With the increase of aging time *rac*-**1** and *rac*-(EBI)Hf(*i*Bu)-(NMe_2) convert to *rac*-(EBI)Hf(iBu)$_2$, and then *rac*-(EBI)Hf(iBu)$_2$ transforms to cationic alkylhafnium species [*rac*-(EBI)Hf(*i*Bu)]$^+$ by the reaction with **2**. The procedure to generate the cationic active species from the reaction of *rac*-**1**, Al(iBu)$_3$, and **2** in this order can thus be summarized as shown in Scheme I.

Previously, hafnocene catalysts were known to show low polymerization activities and to produce high MWs compared with their zirconium analogues because of differences in the concentration of the active centers and different carbon–metal bond strengths.[1m] For example,[1a] the activity of (EBI)$HfCl_2$ (R_p = 610 kg-PP/mol-Hf h C_{mon}) is lower than that of (EBI)$ZrCl_2$ (R_p = 1690 kg-PP/mol-Zr h C_{mon}) by a factor of 3; the activity of Me_2C(Fluo)(Cp)$HfCl_2$ (R_p = 130 kg-PP/mol-Hf h C_{mon}) is lower than Me_2C(Fluo)(Cp)$ZrCl_2$ (R_p = 1550 kg-PP/mol-Zr h C_{mon}) by a factor of 10; the activity of Cp_2HfCl_2 (R_p = 4200 kg-PE/mol-Hf h C_{mon}) is lower than Cp_2ZrCl_2 (R_p = 60,900 kg-PE/mol-Zr h C_{mon}) by a factor of 15. Now we will see this is not true for hafnocene diamide. The activity of present *rac*-**1**/Al(iBu)$_3$/**2** system (R_p = 34,700 kg-PP/mol-Hf h C_{mon}) is much higher than that of (EBI)$HfCl_2$/MAO[1a] or (EBI)$ZrCl_2$/MAO[1a] system, and comparable to that of *rac*-(EBI)Zr(NMe_2)$_2$/Al(iBu)$_3$/**2** system[13] under the similar conditions.

All rate profiles obtained by *rac*-**1**/Al(iBu)$_3$/**2** catalysts are characterized by a rapid increase to maximum rates and then a fast decay to zero rates. The rapid decay of polymerization is caused by either diffusion limitation or accelerating of chain terminations, or the both. The former is caused by a dramatic change of media viscosity and polymer precipitation during the early period of polymerization.[14] The latter is caused by deactivation of the bimolecular process between two catalytic sites,[15] which follows the second-order decay kinetic model.

To understand the alkylation procedure, UV/VIS spectra were recorded by changing the contacting time of *rac*-**1** with Al(iBu)$_3$ in a toluene solution. For comparison, the same spectra were recorded by using the *rac*-(EBI)Zr(NMe_2)$_2$/Al(iBu)$_3$ system. Figure 3 shows the change of spectra of *rac*-**1** during alkylation. As shown in Figure 3(a), *rac*-**1** records two maximums, an intensive and a broad one, at 324 nm and a weaker one at 440 nm. When Al(iBu)$_3$ was introduced

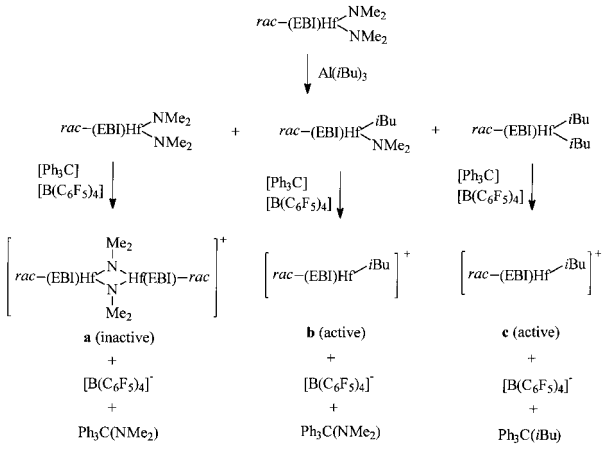

Scheme 1

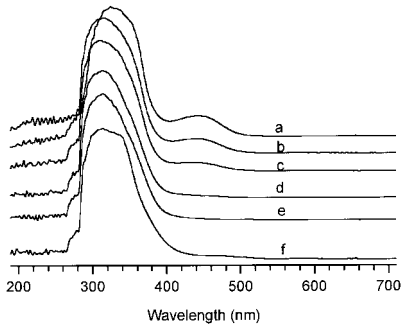

Figure 3 UV/VIS spectra of (a) *rac*-**1,** *rac*-**1**/Al(iBu)$_3$ with different aging times of (b) 1 min, (c) 5 min, (d) 30 min, (e) 420 min, and (f) the *rac*-**1**/Al(iBu)$_3$/**2** system.

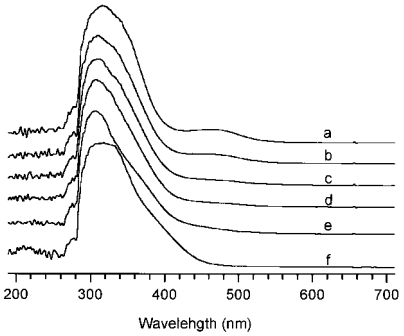

Figure 4 UV/VIS spectra of (a) *rac*-(EBI)$Zr(NMe_2)_2$ and *rac*-(EBI)$Zr(NMe_2)_2$/Al(*i*Bu)$_3$ with different aging times of (b) 1 min, (c) 5 min, (d) 10 min, (e) 420 min, and (f) the *rac*-(EBI)$Zr(NMe_2)_2$/ Al(*i*Bu)$_3$/**2** system.

into the toluene solution containing *rac*-**1**, NMe_2 groups of *rac*-**1** are replaced by *i*Bu groups. The transformation of *rac*-**1** to *rac*-(EBI)Hf(*i*Bu)$_2$ can be traced by the disappearance of the maximum at 440 nm. This band disappears completely after 30 min of alkylation. The zirconium analogue *rac*-(EBI)$Zr(NMe_2)_2$ shows two similar maximums at 316 and 462 nm, as shown in Figure 4(a). The intensity of the maximum at 462 nm decreases sharply within 5 min. According to the maximum at 440 nm (*rac*-**1**) or at 462 nm (*rac*-(EBI)-$Zr(NMe_2)_2$) vs. time plots (Fig. 5), one can see that a longer time is needed for the alkylation of *rac*-**1** than that of *rac*-(EBI)$Zr(NMe_2)_2$.

Effect of $[Ph_3C][B(C_6F_5)_4]$ Concentration

As shown in Figure 1, both activity and lifetime of the active sites increase as the aging time length-

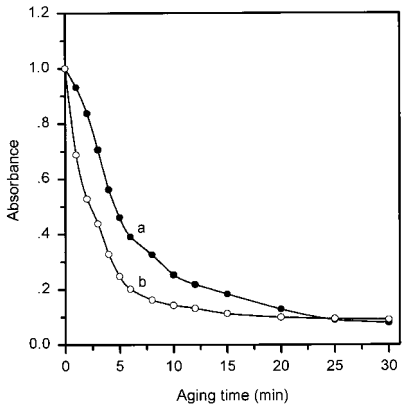

Figure 5 Effect of aging time on intensity of UV/VIS maximum at (a) 440 nm of *rac*-**1**/Al(*i*Bu)$_3$, and (b) 462 nm for *rac*-(EBI)$Zr(NMe_2)_2$/Al(*i*Bu)$_3$.

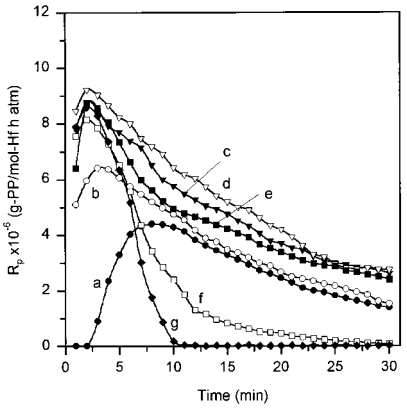

Figure 6 R_p vs. time of propylene polymerization initiated by *rac*-**1**/Al(*i*Bu)$_3$/**2** with [Hf] = 31.3 μM, [Al]/[Hf] = 25, T_p = 50°C, P_{C3H6} = 1.3 atm, and aging time = 1.5 h under different [**2**]/[Hf] ratios of (a) 0.4, (b) 0.5, (c) 0.6, (d) 0.7, (e) 0.8, (f) 1.0, and (g) 1.2.

ens. This indicates that unreacted *rac*-**1** and partially alkylated *rac*-(EBI)Hf(*i*Bu)(NMe_2) exists, together with *rac*-(EBI)Hf(*i*Bu)$_2$, if the aging time is insufficient. The mixture of compounds cannot be completely activated to afford cationic active species by adding 1 equiv. of **2**. To get some information on the active site concentration, propylene polymerization is carried out by changing the concentration of **2**. As can be seen in Figure 6, the polymerization rate profiles changes very much as the [**2**]/[*rac*-**1**] ratio changes from 0.4 to 1.2. When the [**2**]/[*rac*-**1**] ratio changes from 0.4 to 0.7, the activity increases almost linearly, and the lifetime of the active sites lengthens from 40 min to more than 1 h. When [**2**]/[*rac*-**1**] increases from 0.7 to 1.2, all polymerizations increase to similar $R_{p,\max}$ values and then decrease quickly, and the lifetime of the active sites becomes shorter. Figure 7 plots the $\overline{R_p}$ and $R_{p,\max}$ vs. the [**2**]/[*rac*-**1**] ratio. Both $\overline{R_p}$ and $R_{p,\max}$ values show maximum at [**2**]/[*rac*-**1**] = 0.7. The $\overline{R_p}$ vs. the [**2**]/[*rac*-**1**] plot shows a bell-shape curve, while $R_{p,\max}$ stays almost unchanged when [**2**]/[*rac*-**1**] > 0.6.

Bochmann[16] has studied the detailed NMR-scale reactions between *rac*-$Me_2Si[Ind]_2ZrMe_2$ and **2** in weakly coordinating solvents such as dichloromethane or toluene. In the presence of 0.5 equiv. of Al_2Me_6, *rac*-$Me_2Si[Ind]_2ZrMe_2$ and **2** react to afford the heterodinuclear dimeric complex [*rac*-$Me_2Si[Ind]_2Zr(\mu\text{-}Me)_2AlMe_2]^+$, the adduct of the base-free [*rac*-$Me_2Si[Ind]_2Zr(Me)]^+$ cation, and $AlMe_3$. However, the formation of these dimeric species may not be relevant to the present

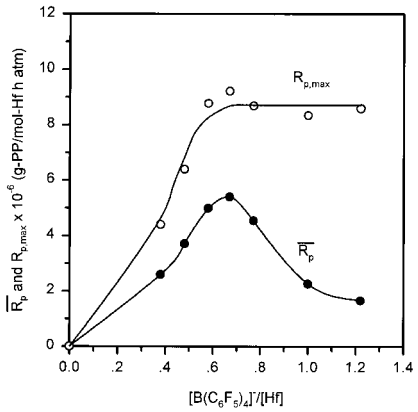

Figure 7 R_p and $R_{p,\max}$ vs. concentration of **2.** The polymerization conditions as in Figure 6.

catalytic system, because *rac*-**1**/Al(iBu)$_3$/**2** system carries much longer alkyl chains whose bulkiness would prevent the formation of the heterodinuclear species. There is no information about the coordination mode of longer alkyl ligands in cationic complexes.

If *rac*-**1** is not completely alkylated by Al(iBu)$_3$, three kinds of precursors, *rac*-(EBI)Hf(iBu)$_2$, *rac*-(EBI)Hf(iBu)(NMe$_2$), and unreacted *rac*-**1**, exists before activation with **2**. Upon introducing **2** into the mixture, each compound transforms into the cationic complexes, as already shown in Scheme I. At low concentration of **2**, say [**2**]/[Zr] = 0.4, it may be assumed that the completely alkylated compound *rac*-(EBI)Hf(iBu)$_2$ is selectively reacted with **2** to afford [*rac*-(EBI)Hf(iBu)]$^+$ cations and the Ph$_3$C(iBu) by-product, so that polymerization carried out at this low concentration of **2** shows fairly high activity [Fig. 6(a)]. As [**2**] increases, *rac*-(EBI)Hf(iBu)(NMe$_2$) and *rac*-**1** can also form cationic species, [*rac*-(EBI)Hf(iBu)]$^+$ and [*rac*-(EBI)Hf(NMe$_2$)]$^+$ (Scheme I). The cationic complex [*rac*-(EBI)Zr(NMe$_2$)]$^+$ containing an amide has already been reported to be generated from the reaction of *rac*-(EBI)Zr(NMe$_2$)$_2$, 2 Al$_2$Me$_6$, and [HNR$_3$][B(C$_6$F$_5$)$_4$].[17] However, HNMe$_2$ generated during the reaction is coordinated strongly to the Zr center, resulting in no activity in the polymerization. Even if the generation of HNMe$_2$ may be avoided by using **2** instead of ammonium salts, [*rac*-(EBI)Hf(NMe$_2$)]$^+$ cations are most probably transformed to more stable dimeric cation **a** in Scheme I. In addition, the Ph$_3$C(NMe$_2$) by-product may also be coordinated to [*rac*-(EBI)Hf(iBu)]$^+$ cations strong enough to influence the catalytic activity and to [*rac*-(EBI)Hf(NMe$_2$)]$^+$ cations as a stabilizer.

According to the polymerization results shown in Figure 7, the generation of cationic species from *rac*-(EBI)Hf(iBu)(NMe$_2$) and *rac*-**1** is not so significant when [**2**]/[*rac*-**1**] ratio is below 0.8. However, as the ratio increases above 1.0, all catalytic precursors are activated to afford active (**b** and **c** in Scheme I) or inactive (**a**) cationic species. The rapid decay of polymerization after reaching similar $R_{p,\max}$ at [**2**]/[*rac*-**1**] > 1.0 might be related with the activation of the precursors containing amide as ligands: the [*rac*-(EBI)Hf(NMe$_2$)]$^+$ cations are deactivated by dimerization and part of [*rac*-(EBI)Hf(iBu)]$^+$ cations are deactivated by the coordination of amine byproducts.

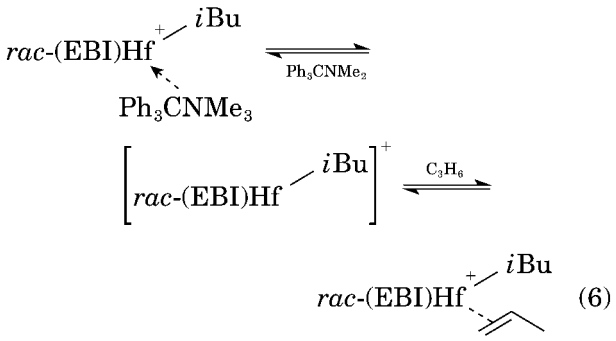

An excess amount of **2** will produces more of a —NMe$_2$ group, which leads to the equilibrium to the inactive left species of eq. (6).

Effect of AlR$_3$

Propylene polymerizations were carried out for 30 min by using AlR$_3$/**2** or methylaluminoxane (MAO) as a cocatalyst at polymerization temperature (T_p) of 50°C. Various types of AlR$_3$ such as Al(iBu)$_3$, Al(iBu)$_2$H, AlEt$_3$, and AlMe$_3$ have been investigated. Figure 8 is the polymerization rate profiles obtained by using *rac*-**1**/Al(iBu)$_3$/**2** system. The rates quickly increase to maximum activities without an induction period [except Fig. 8(a)] and then decay fast. The lifetime of the active sites are no more than 30 min because of the short aging time and high [**2**]/[*rac*-**1**] ratio. The polymerizations keep high activities within a rather narrow [Al]/[*rac*-**1**] molar ratio, and highest activity can be found when [Al]/ [*rac*-**1**] = 25.

Propylene polymerizations were also carried out by using the *rac*-**1**/Al(iBu)$_2$H/**2** system (Fig. 9). The polymerization profiles are changed very much by changing the concentration of Al(iBu)$_2$H.

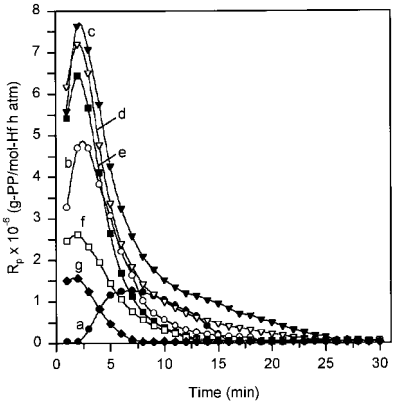

Figure 8 R_p vs. time plots of polypropylene polymerization initiated by *rac*-**1**/Al(iBu)$_3$/**2** with [Hf] = 31.3 μM, [**2**]/[Hf] = 1.0, T_p = 50°C, P_{C3H6} = 1.3 atm, and aging time = 0.5 h under different [Al]/[Hf] ratios of (a) 5, (b) 13, (c) 25, (d) 40, (e) 52, (f) 78, and (g) 110.

It seems that lower [Al] benefits higher activity, but the deactivation is very severe, resulting in a short lifetime of active sites. It is interesting to note that the deactivation becomes insignificant and the induction period becomes longer at high [Al]/[*rac*-**1**] ratios. Considering *ansa*-metallocene diamide compounds are easily alkylated by using a common AlR_3, *rac*-**1** can react with Al(iBu)$_2$H to afford the corresponding metallocene dihydride compound:

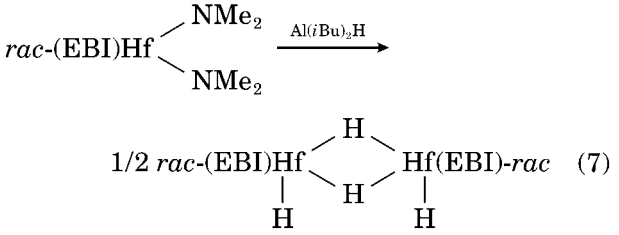

(7)

The complex Cp_2MH_2 (M = Zr or Hf) has been extensively characterized by ^{1}H-NMR spectral studies, and has been shown to adopt a dimeric structure with bridging and terminal hydrido ligands in both a benzene-d_6 and toluene-d_8 solution.[18,19] The chemistry of Cp_2MH_2 has been extensively reviewed.[20] In particular, it is well known that these species react readily with unsaturated organic functions. In the present study we introduced propylene monomer into the reactor after reacting *rac*-**1** with Al(iBu)$_2$H, so that propylene may be inserted into an unstable Hf—H bond.

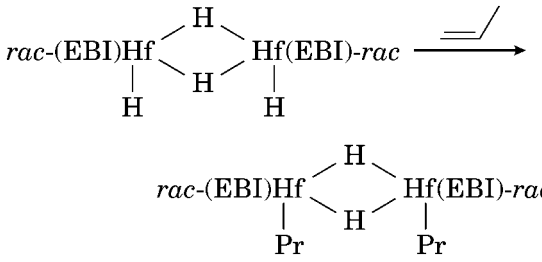

(8)

A similar structure [{ZrR(μ-H)(ηh-C_5H_5)$_2$}$_2$] has been demonstrated by Lappert et al.,[20] and the binuclear species react with **2** in the presence of excess Al(iBu)$_2$H to afford heterodinuclear cationic species [*rac*-(EBI)Hf(μ-H)$_2$Al(iBu)$_2$]$^+$. A similar [*rac*-(EBI)Zr(μ-Me)$_2$AlMe$_2$]$^+$ cation has been identified from the reaction of the *rac*-(EBI)Zr(NMe$_2$)$_2$/**2** Al_2Me_6/[HNR_3][$B(C_6F_5)_4$] system.[17] The cationic complex [*rac*-(EBI)Hf(μ-H)$_2$Al(iBu)$_2$]$^+$ may undergo loss or displacement of Al(iBu)$_2$H, ultimately leading to *rac*-[(EBI)ZrH]$^+$, and then to the [*rac*-(EBI)Zr(Pr)]$^+$ species by the insertion of propylene to the Hf—H bond. In the presence of an excess amount of Al(iBu)$_2$H the formation of the base-free [*rac*-(EBI)Zr(Pr)]$^+$ cations might be restricted due to the equilibrium shown in eq. (10), resulting in low $R_{p,max}$ values at high [Al]/[Hf] ratios (Fig. 9).

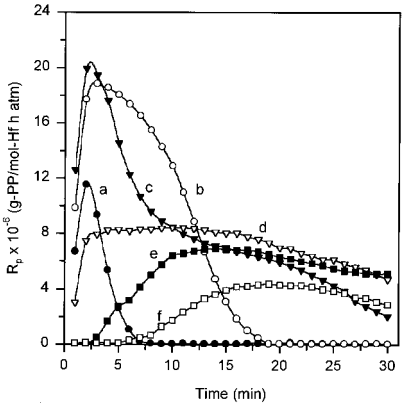

Figure 9 R_p vs. time plots of polypropylene polymerization initiated by *rac*-**1**/Al(iBu)$_2$H/**2** with [Hf] = 31.3 μM, [**2**]/[Hf] = 1.0, T_p = 50°C, P_{C3H6} = 1.3 atm, and aging time = 1.5 h under different [Al]/[Hf] ratios of (a) 24, (b) 36, (c) 42, (d) 48, (e) 60, and (f) 96.

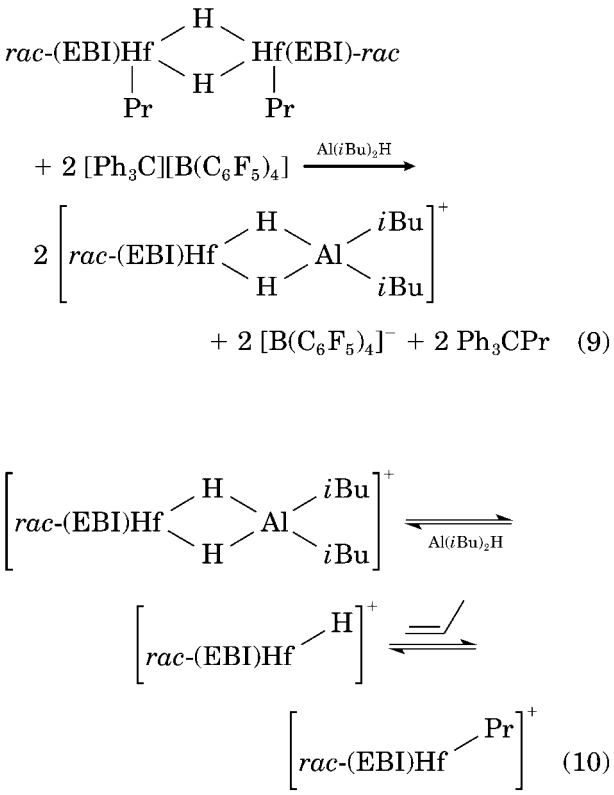

The other two kinds of common alkylaluminum, $AlEt_3$ and $AlMe_3$, were also used as an alkylating reagent of *rac*-**1**. The detailed polymerization conditions are: [*rac*-**1**] = 31.3 μM, [Al]/[*rac*-**1**] = 24, [**2**]/[*rac*-**1**] = 0.6, aging time = 1.5 h, T_p = 50°C, and P_{C3H6} = 1.3 atm. The activity of polymerization is recorded as 0.10×10^6 (g-PP/mol-Hf h atm) for the *rac*-**1**/$AlEt_3$/**2** system. However, the *rac*-**1**/$AlMe_3$/**2** system shows only negligible activity at the above conditions. The negligible activity of the *rac*-**1**/$AlMe_3$/**2** system may be due to the fact that in the presence of $AlMe_3$, the cations [*rac*-(EBI)-HfMe]$^+$ preferentially form the heterodinuclear complexes [*rac*-(EBI)Hf(μ-Me)$_2$AlMe$_2$]$^+$ in toluene solvent [see eq. (4)]. E quilibrium exists between [*rac*-(EBI)HfMe]$^+$ and [*rac*-(EBI)Hf(μ-Me)$_2$AlMe$_2$]$^+$ during the reaction. The $AlMe_3$ adduct [*rac*-(EBI)Hf(μ-Me)$_2$AlMe$_2$]$^+$ is coordinatively saturated and lacks a vacant orbital suitable for binding the propylene monomer. Initiation of chain growth, therefore, requires the dissociation of the $AlMe_3$ to [*rac*-(EBI)HfZrMe]$^+$, but in the presence of a small $AlMe_3$, the equilibrium may favor the heterodinuclear complexes. There is a similar case for *rac*-**1**/$AlEt_3$/**2** system. Bochmann did the propylene polymerization with the system *rac*-$Me_2Si(Ind)_2ZrMe_2$/AlR_3/**2** in the presence of 1 to 500 equivalents of $AlEt_3$[21] or AlMe.[16,22] The highest activity were found for an [$AlEt_3$]/[Zr] ratio of 10 : 1 and an [$AlMe_3$]/[Zr] ratio of only 1 : 1. Based on this result and detailed spectroscopic results, Bochmann concluded that, in the presence of $AlEt_3$ or $AlMe_3$, the heterodinuclear complexes [*rac*-$Me_2Si(Ind)_2Zr(\mu\text{-}R)_2AlR_2$]$^+$ (R = Me, Et) are major cationic species.

In summary the bulkier isobutyl substituents may render inactive heterodinuclear complexes sterically unfavorable, and this could result in a higher number of active sites. In addition, the bulkiness of isobutyl substituents gives rise to more separated ion pairs, and this facilitates the access of the monomers to the active sites. However, as the bulkiness of the substituents decreases as in the case of ethyl and methyl, the equilibrium of cationic species is inclined to direct to inactive heterodinuclear species, resulting in low activity. The activity of the *rac*-**1**/AlR_3/**2** system is deeply influenced by the type of AlR_3 and decreased in the order: $Al(iBu)_2H$ > $Al(iBu)_3$ > $AlEt_3$ > $AlMe_3$.

MAO has been one of the most efficient cocatalyst. According to the propylene polymerizations carried out by the *rac*-**1**/MAO system with polymerization conditions of: [*rac*-**1**] = 31.3 μM, aging time = 24 h, T_p = 50°C, P_{C3H6} = 1.3 atm, and [Al]/[Hf] = 100 to 10,000, MAO is not an efficient activator for *rac*-**1**. Very low activity (0.40×10^6 g-PP/mol-Hf h atm) is recorded when the [Al]/[Hf] ratio is 10,000. The activity of *rac*-**1**/MAO is almost negligible when the [Al]/[Hf] ratio is below 10,000. The low activity seems to be deeply related with free $AlMe_3$ unavoidably contained in MAO.

Effect of Polymerization Temperature (T_p)

Propylene polymerization initiated by *rac*-**1**/$Al(iBu)_3$/**2** have been carried out at the T_p range from 30 to 90°C (Fig. 10). All polymerizations rise to maximum rates within 5 min, and then decrease quickly to a zero rate in 30 min. The rapid decay of polymerization is possibly due to both the chemical deactivation of catalytic active sites and the diffusion limitation of the propylene monomer caused by the dramatic change of viscosity of reaction medium during the early stage of polymerization. The polymerization carried out by a similar catalytic system *rac*-(EBI)$Zr(NMe_2)_2$/$Al(iBu)_3$/**2**[13] decayed not as fast as those by the *rac*-**1**/$Al(iBu)_3$/**2** system. The former system pro-

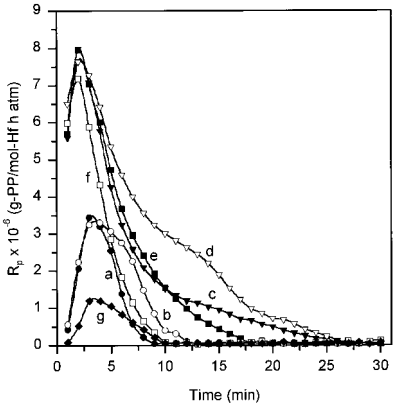

Figure 10 R_p vs. time plots of polypropylene polymerization initiated by *rac*-**1**/Al(iBu)$_3$/**2** with [Hf] = 31.3 μM, [Al]/[Hf]/[**2**] = 25/1/1, P_{C3H6} = 1.3 atm, and aging time = 0.5 h under different polymerization temperatures of (a) 30 (b) 40, (c) 50, (d) 60, (e) 70, (f) 80, and (g) 90°C.

duces a polymer with a lower molecular weight than the latter system by an order of magnitude, so that the high molecular weight of the polymer obtained by the latter system seems to be deeply related with the rapid decay of polymerization.

Early in the study of Ziegler-Natta catalysts the coordination-anionic mechanism for olefin polymerization with these catalysts was proposed,[23,24] and it is widely accepted to be the mechanism of propagation in metallocene catalysis as well. According to this mechanism the addition of monomer to a polymer chain consists of two consecutive steps: (i) the coordination of an olefin monomer with the transition metal atom of an active site, i.e., the reversible formation of π-complex; and (ii) the insertion of the olefin monomer between the metal atom and the growing polymer chain.

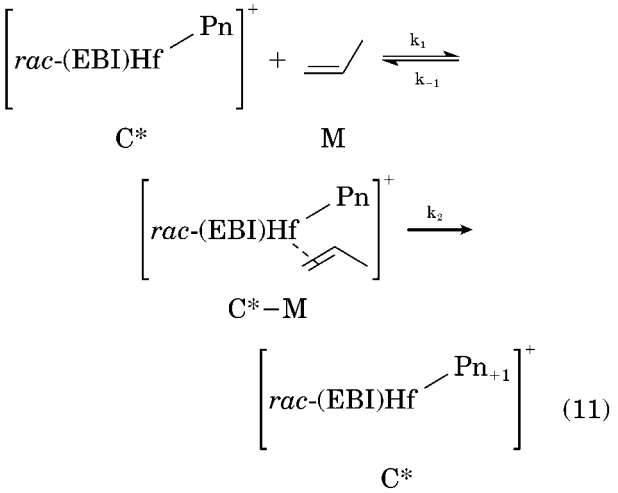

(11)

In this equation, k_1, k_{-1}, and k_2 are the rate constants, C^* is a cationic active site of catalyst, M is a propylene monomer, and C^*-M is a cationic alkyl propylene intermediate. The pseudo-steady-state expression for the polymerization rate can be expressed by eq. (12), by assuming that Hf^+-P_n and Hf^+-P_{n+1} are kinetically indistinguishable, $d[C^*\text{-}M]/dt = 0$, and $[C^*]_0 = [C^*] + [C^*\text{-}M]$.

$$R_p = [C^*]_0(k_1k_2[M])/(k_1[M] + k_{-1} + k_2) \quad (12)$$

This is the same as the standard equation to express the initial reaction velocity for the simplest enzyme reaction, if the monomer coordinates to the propagating sites is strong, $k_1[M] >> k_{-1} + k_2$. In this case,

$$R_p = k_2[C^*]_0 \quad (13)$$

i.e., the rate of polymerization is independent of $[M]$, which contradicts experimental findings.[1a,27,28] In addition, the cationic alkyl propylene π-complex is expected to be unstable at the T_p range of this study. If the strength of monomer coordination is very weak, $k_{-1} >> k_1[M]$. In this case, eq. (12) is simplified as,

$$R_p = [C^*]_0(k_1k_2[M])/(k_{-1} + k_2) \quad (14)$$

where the effective rate constant $k_{eff} = k_1k_2/(k_{-1} + k_2)$. The Arrhenius plots of activity ($R_{p,max}$) are linear over the entire range of T_p for both catalysts (Fig. 11). We chose the $R_{p,max}$ value as an activity for the plots, because all polymerizations rise to $R_{p,max}$ within a few minutes of polymeriza-

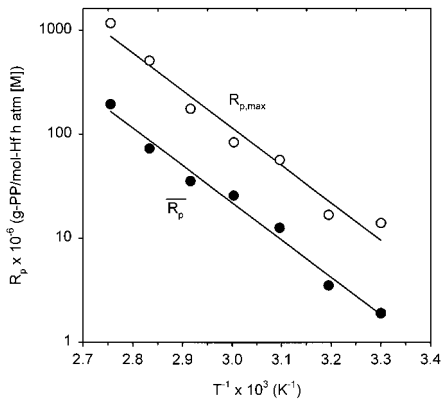

Figure 11 Arrhenius plot of polymerization rate for propylene polymerization.

tion so that it can be assumed to be the initial rates. Here, $R_{p,\max}$ is given g PP per mol of Hf per hour per mol of propylene monomer.[25] From the slope of Figure 11, the overall activation energy is calculated as 7.14 kcal/mol.

If the insertion of the propylene monomer between the metal atom and the growing polymer chain is much faster than the dissociation of the monomer from the π-complex, i.e., $k_2 >> k_{-1}$, eq. (14) can be simplified as,

$$R_p = [C^*]_0(k_1/k_{-1})[M] \quad (15)$$

In this case, the equilibrium constant of the first step in eq. (11) plays a major role in determining the rate of polymerization.

Characterization of Polymer

The properties of polymers obtained in this study are summarized in Table I, together with the catalytic activity data. The molecular weight (MW) of polymer produced at low T_p (30°C) is very high (M_v = 387,300). The MW of the polymer decreases monotonically as T_p increases. This is a typical phenomenon found in the olefin polymerizations by a metallocene catalyst. Ewen et al.[26] reported that the molecular weight of PP produced by *rac*-(EBI)$HfCl_2$, *rac*-(EBTHI)$HfCl_2$ (EBTHI = Et$(IndH)_4$) showed a decrease with increasing polymerization temperature. The typical isospecific *rac*-(EBI)$HfCl_2$ and syndiotactic Me_2C(Flu)(Cp)$HfCl_2$ catalyst produce polypropylene with M_v = 446,000 and 750,000 g/mol, respectively.[1a]

The *i*PP samples are characterized by a narrow molecular weight distribution (MWD), which is the great promise of metallocene catalysts. It is interesting to note that MWD becomes narrow from 2.90 to 2.10 when T_p increases from 30 to 90°C. The MWD is not as sensitive to temperature. Even if the decrease of the MWD value with T_p has been reported for both ethylene[27] and propylene[28] polymerization by Cp_2ZrCl_2/MAO catalysts, as well as propylene polymerization by the *rac*-$Me_2Si(1\text{-}C_5H_2\text{-}2\text{-}CH_3\text{-}4\text{-}tBu)_2Zr(NMe_2)_2$ catalyst.,[15a,c] it is not as easy to interpret the data. To understand the unexpected decrease of MWD according to T_p, fractionations of polymers have been performed with the samples obtained at different T_p, and the results are shown in Table II. Three kinds of polymer samples are fractionated by refluxing with ethyl ether (E), *n*-pentane (C_5), *n*-hexane (C_6), and *n*-heptane (C_7) sequentially. The amount of remained fraction (C_7 insoluble) decreases form 82.0 to 51.9% as T_p increases from 30 to 50°C. The GPC curve of the polymer produced at T_p = 30°C showed a conspicuous tail of a high MW fraction. This means that this sample is compositionally inhomogeneous. It is very interesting to note that polymer produced at T_p = 70°C is solely soluble into *n*-pentane, demonstrating that the polymer is compositionally very homogeneous. Thus, the decrease of MWD at high T_p might be caused by the compositional homogeneity.

The [*mmmm*] value of the polymer decreases monotonously as T_p increases, and the sample produced at 90°C shows an atatic feature ([*mmmm*] = 44%). Generally *ansa*-metallocene complexes in solution are rather soft. The thermal disturbance at raised T_p causes a strong vibration of ligands and the deformation of their rigid confirmation, which results in the loss of their stereoregulating ability.

Both MW and [*mmmm*] values of polymers decrease as aging time and anion concentration increase. As aging time or anion concentration increase, all metallocenes react with cocatalyst components to form cationic active species, resulting in the increase of the concentration of the active sites, especially at the early stage of polymerization. The increase of the cationic sites may give them more opportunities for the bimolecular reversible deactivation, resulting in the decrease of MW. The complicated equilibria formed during the early stage of polymerization at a high anion concentration (*vide supra*) cause low isotacticity of the polymer.

The MW values of polymers produced by both *rac*-**1**/Al(*i*Bu)$_3$/**2** and *rac*-**1**/Al(*i*Bu)$_2$H/**2** systems slightly increase at a very low [Al]/[Hf] ratio to reach maximum, and then declines with additional AlR_3. The isotacticity of polymers is high when the [Al]/[Hf] ratio is low or high. These results demonstrate that the effect of AlR_3 on MW isospecificity is very complex. AlR_3 acts as a lewis acid to enhance the propagation rate, bur it can react with the catalyst to terminate the reaction as well. In addition, AlR_3 can coordinate to the catalyst to slow the propagation rate by reversible inhibition. This may result in the maximum MW at some AlR_3 concentration. The MW values of polymers produced by *rac*-**1**/Al(*i*Bu)$_3$/**2** is slightly larger than those of polymer by the *rac*-**1**/Al(*i*Bu)$_2$H/**2** system, even if the isospecificity of

Table I Characterization of *i*PP Produced by *rac*-1 with Different Cocatalysts[a]

Run No.	[Hf] (μmol/L)	Cocatalyst	[Al]/[Hf]	**2**/[Hf]	T_p (°C)	Aging Time (h)	$\overline{R_p}$[b] $\times 10^{-6}$	[*mmmm*] (%)	$\overline{M_v} \times 10^{-4}$	$\overline{M_w} \times 10^{-4}$	$\overline{M_w}/\overline{M_n} \times 10^{-4}$	T_m (°C)	X_C[d] (%)
Figure 10(a)					30		1.91[c]	89.2	38.73	51.61	2.90	135.2	24.1
Figure 10(b)					40		3.52[c]		27.77			131.1	31.6
Figure 10(c)					50		12.6[c]	83.7	16.63	22.86	2.35	127.8	30.7
Figure 10(d)	31.3	Al(*i*Bu)$_3$/**2**	25	1.0	60	0.5	25.9[c]		6.03			118.7	29.0
Figure 10(e)					70		35.6[c]	71.2	4.26	5.47	2.15	111.8	24.0
Figure 10(f)					80		72.9[c]		4.04			88.7	18.6
Figure 10(g)					90		194.9[c]	44.6	0.83	1.03	2.10	66.1	1.5
Figure 1(a)						1min	0.68		18.36			129.1	34.5
Figure 1(c)						1.5	2.26	86.7	17.47			127.5	33.9
Figure 1(d)	31.3	Al(*i*Bu)$_3$/**2**	25	1.0	50	2.5	3.06		16.32	24.12	3.49	125.0	30.0
Figure 1(e)						4.0	4.26	82.7	12.81			124.2	28.3
Figure 1(f)						7.0	4.64		11.29			122.8	32.7
Figure 1(g)						12.0	4.19	82.5	11.36			122.7	28.7
Figure 6(a)				0.4			2.60	85.5	17.38			127.8	34.0
Figure 6(b)				0.5			3.71		15.58			127.2	29.8
Figure 6(c)	31.3	Al(*i*Bu)$_3$/**2**	25	0.6	50	1.5	4.99	83.7	14.77			125.7	29.6
Figure 6(d)				0.7			5.40		13.65			124.9	32.0
Figure 6(e)				0.8			4.54	83.8	13.47			124.4	30.8
Figure 6(g)				1.2			1.66	81.3	9.87			122.5	27.8
Figure 8(a)			5				0.37	86.0	19.18	29.42	4.02	128.2	23.4
Figure 8(b)			13				0.79		19.34			128.6	27.6
Figure 8(c)			25				1.74	83.7	16.63	22.86	2.35	127.8	30.7
Figure 8(d)	31.3	Al(*i*Bu)$_3$/**2**	39	1.0	50	0.5	1.35		16.79			126.6	31.6
Figure 8(e)			52				0.97	84.9	15.36			127.4	32.0
Figure 8(f)			78				0.47	86.6	15.28			129.9	26.6
Figure 8(g)			110				0.22		14.84			127.2	20.7
Figure 9(a)			25				1.25	86.1	12.35	14.54	2.98	129.0	32.2
Figure 9(b)			36				6.57		12.98			128.4	26.0
Figure 9(c)	15.6	Al(*i*Bu)$_2$H/**2**	42	0.6	50	1.5	8.04	83.6	14.60	17.99	3.15	128.6	29.3
Figure 9(d)			48				7.11	83.6	14.08			129.3	25.8
Figure 9(e)			60				5.03		13.85			129.2	32.2
Figure 9(f)			96				2.62	86.5	12.56			130.9	36.9
1	31.3	Al(*i*Bu)$_2$H/**2**	25	0.6	50	1.5	2.40	86.0	13.06			126.9	35.2
2	31.3	AlEt$_3$/**2**	25	0.6	50	1.5	0.10	88.5	1.86	2.85	1.78	132.8	31.5
3	31.3	MAO	10,000	—	50	24	0.26	88.7	1.55			129.9	10.2

[a] Polymerization conditions are given in correspondence figures shown in run number.
[b] Unit of polymerization rate is given in g-PP (mol-Hf)$^{-1}$ h^{-1} atm^{-1}.
[c] Unit of R_p is g-PP (mol-Hf)$^{-1}$ h^{-1} atm^{-1} $[M]^{-1}$.
[d] X_C: Crystallinity calculated by $X_C = (\Delta H_f/\Delta H_f^0) * 100$; ΔH_f = the heat of fusion of the sample by DSC; ΔH_f^0 = heat of fusion for folded-chain PP.

Table II Fractionation of iPP Obtained under Different T_p[a]

Run No.	T_p (°C)	Fraction	wt % Polymer in Fraction	T_m (°C)	$\overline{M_v} \times 10^{-4}$
Figure 10(a)	30	Total	100	135.2	38.73
		E	0		
		C_5	0		
		C_6	0.9	—	—
		C_7	17.1	136.2	37.97
		Remained	82.0	137.2	39.12
Figure 10(c)	50	Total	100	127.8	16.63
		E	0		
		C_5	3.0	124.8	—
		C_6	2.1	127.9	—
		C_7	43.0	131.8	14.10
		Remained	51.9	133.3	19.57
Figure 10(e)	70	Total	100	111.8	4.26
		E	0		
		C_5	100	111.9	4.17
		C_6	0		
		C_7	0		

[a] Polymerization conditions are given corresponding to the figure shown in run number.

both systems is almost the same. It is interesting to note that the polymers produced by *rac*-**1**/$AlEt_3$/**2** and *rac*-**1**/MAO catalysts show very low MW values due to the enhanced termination and/or chain transfer.

The melting temperature (T_m) and crystallinity of polymers decreases with the increase of T_p. The T_m values of polymers are also slightly decreased as the aging time and the [**2**]/[*rac*-**1**] ratio increases, and the variation of the T_m according to the [Al]/[Hf] ratio is almost in line with the change of the [*mmmm*] value. The melting points and the crystallinities of *i*PPs produced in this study are at a similar level with those obtained with the *rac*-(EBI)$HfCl_2$/MAO system.[26]

CONCLUSION

The *ansa*-hafnocene amide compound *rac*-**1** can be used directly in catalyst formulations without conversion to a dichloride complex or a dialkyl complex. The MAO-free system *rac*-**1**/Al(*i*Bu)$_3$/**2** is much more effective than the *rac*-**1**/MAO system for the propylene polymerizations, and the activity of the *rac*-**1**/Al(*i*Bu)$_3$/**2** system is higher than that of the (EBI)$HfCl_2$/MAO[1a] or (EBI)$ZrCl_2$/MAO[1a] system, and almost same as that of the *rac*-(EBI)Zr(NME_2)$_2$/Al(*i*Bu)$_3$/**2** system[13] under the similar conditions. The UV/VIS measurement give evidence that alkylating *rac*-**1** to *rac*-(EBI)-HfR_2 needs more time than the corresponding zirconocene analogue. The activity increases by a factor of 7 by increasing the aging time from 1 min to more than 4 h.

The activity of the *rac*-**1**/Al(*i*Bu)$_3$/**2** catalyst is very sensitive to the type and concentration of AlR_3, and decreases in the order: Al(*i*Bu)$_2$H > Al(*i*Bu)$_3$ > $AlEt_3$ > $AlMe_3$. The catalyst keeps high activity in a narrow range of the [Al]/[Hf] ratio. The use of MAO is not very efficient for activating the catalyst *rac*-**1**. In addition, the activity is influenced by the concentration of **2**, and as a result, the maximum activity is observed when **2**/*rac*-**1** = 0.7. The activity of the *rac*-**1**/AlR_3/**2** catalyst is also sensitive to the polymerization temperature. The maximum and overall polymerization rates vs. T_p plots obey the Arrhenius relation. The activation energy for the overall reactions are caculated as 7.14 kcal/mol.

The properties of polymer such as isotacticity (as [*mmmm*]), MW, MWD, T_m, and crystallinity, are at a similar level with those obtained with the *rac*-(EBI)$HfCl_2$/MAO system.[26] The MW and isotacticity of the polymer produced by the MAO-free system decreases monotonically as T_p increases, and MWD becomes narrow from 2.90 to 2.10 when T_p increaces from 30 to 90°C because of the

compositional homogeneity of the polymer produced at high T_p, which is demonstrated by fractionation of the polymer. Both MW and [*mmmm*] values of polymers decrease as aging time and anion concentration increase. The MW values of polymers produced by both *rac*-**1**/Al(iBu)$_3$/**2** and *rac*-**1**/Al(iBu)$_2$H/**2** catalysts slightly increase at a very low [Al]/[Hf] ratio to reach maximum, and then declines with additional AlR_3.

Acknowledgement is made to the donors of the Korea Research Foundation (Nondirected Fund, 1997). The authors are grateful to Mr. Jinkee Sung (the Korea Petrochemical Co.) for arranging the GPC analysis, and Dr. M.-S. Won for arranging the ^{13}C-NMR analysis.

REFERENCES

1. (a) Kaminsky, W. Macromol Chem Phys 1996; 197, 3907; (b) Olagoke, O.; Muhammad, A.; Kaminsky, K. J Macromol Sci Rev Macromol Chem Phys 1997; C37, 519; (c) Ribeiro, M. R.; Deffieux, A.; Portela, M. F. Ind Eng Chem Res 1997, 36, 1224; (d) Thayer, A. M.; Chem Eng News 1995; 73, 15; (e) Brintzinger, H. H.; Fischer, D.; Mlhaupt, R.; Rieger, B.; Waymouth, R. M. Angew Chem Int Ed Engl 1995; 34, 1143; (f) Sinclair, K. B.; Wilson, R. B. Chem Ind 1994, 857; (g) Mhring, P. C.; Coville, N. J. J Organomet Chem 1994, 479, 1; (h) Stehling, U.; Diebold, J.; Kirsten, R.; Rll, W.; Brintzinger, H. H.; Jungling, S.; Mlhaupt, R.; Langhauser, F. Organometallics 1994, 13, 964; (i) Spaleck, W.; Kuber, F.; Winter, A.; Rohrmann, J.; Bachmann, B.; Antberg, M.; Dolle, V.; Paulus, E. F. Organometallics 1994; 13, 954; (j) Horton, A. D. Trends Polym Sci 1994; 2, 158; (k) Farina, M. Trends Polym Sci 1994, 2, 80; (l) Bochmann, M. Nachr Chem Tech Lab 1993; 41, 1220; (m) Kaminsky, W.; Engehausen, R.; Zoumis, K.; Spaleck, W.; Rohrmann, R. Makromol Chem 1992, 193, 1643; (n) Ewen, J. A.; Elder, M. J.; Jones, R. L.; Haspeslagh, L.; Atwood, J. L.; Bott, S. G.; Robinson, K. Makromol Chem Macromol Symp 1991; 48/49, 253.
2. Kaminsky, W.; Klper, K.; Brintzinger, H. H.; Wild, F. R. W. P. Angew Chem 1985, 97, 507.
3. Kaminsky, W. Angew Makromol Chem 1986, 145/146, 149.
4. Kaminsky, W.; Schlobohm, M. Makromol Chem Macromol Symp 1986, 4, 103.
5. Ewen, J. A.; Haspeslagh, L.; Atwood, J. L.; Zhang, H. J Am Chem Soc 1987, 109, 6544.
6. Collins, S.; Kuntz, B. A.; Taylor, N. J.; Ward, D. G. J Organomet Chem 1988, 342, 21.
7. Grossman, R. B.; Doyle, R. A.; Buchwald, S. L. Organometallics 1991, 10, 1501.
8. Buchwald, S. L.; Grossman, R. B. U.S. Pat. 5004820 (1991).
9. (a) Diamond, G. M.; Jordan, R. F.; Petersen, J. L. J Am Chem Soc 1996; 118, 8024; (b) Diamond, G. M.; Jordan, R. F.; Petersen, J. L. Organometallics 1996, 15, 4030, 4045; (c) Christopher, J. N.; Diamond, G. M.; Jordan, R. F.; Petersen, J. L. Organometallics 1996, 15, 4038.
10. Bochmann, M.; Lancaster, S. L. J Organomet Chem 1992, 434, C1.
11. Krigbaum, W. R.; Uematsu, I. J Polym Sci Part A 1965, 3, 767.
12. Chang, R. J Polym Sci 1957, 28, 235.
13. Kim, I.; Hwang, G. N.; Choi, C. S. manuscript in preparation.
14. Tait, P. J. T.; Monteiro, M. G. K. MetCon '95, Houston, TX, 1995.
15. (a) Chien, J. C. W. J Am Chem Soc 1959, 81, 86; (b) Zhou, J. M.; Kim, I. J Polym Sci submitted; (b) Zhou, J. M.; Kim, I. Macromol Chem Phys submitted.
16. (a) Bochmann, M. Polymeric Materials Encyclopedia; Salamon, J. C., Ed.; CRC Press, Boca Raton, FL, p. 4177, vol. 6; (b) Bochmann, M.; Lancaster, S. J. Angew Chem Int Ed Engl 1994, 33, 1634.
17. Kim, I. J Macromol Sci Pure Appl Chem 1998, A35.
18. Bickley, D. G.; Hao, N.; Bougeard, P.; Sayer, B. G.; Burns, R. C.; McGlinchey, M. J.; J Organomet Chem 1983, 246, 257.
19. Jones, S. B.; Peterson, J. L. Inorg Chem 1981, 20, 2889.
20. (a) Jeffery, J.; Lappert, M. F.; Luong-Thi, N. T.; Webb, M.; Atwood, J. L.; Hunter, W. E. J Chem Soc Dalton Trans 1981, 1593; (b) Wilkinson, S. G.; Gordon, F.; Stone, A.; Abel, E. W. Comprehensive Organometallic Chemistry; Pergamon Press: New York, 1982, p. 559, vol. 3.
21. Bochmann, M.; Lancaster, S. J. J Organomet Chem 1995, 497, 55.
22. Bochmann, M.; Lancaster, S. J. Angew Chem 1994, 106, 1715.
23. Cossee, P. J Catal 1964, 3, 80.
24. Ivin, K.; Rooney, J.; Stewart, C.; Green, M.; Mahtab, R. J Chem Soc Chem Commun 1978, 604.
25. Rieger, B.; Mu, X.; Mallin, D. T.; Chien, J. C. W. Macromolecules 1990, 23, 3559.
26. Ewen, J. A.; Haspeslagh, L.; Elder, M. J.; Atwood, J. L.; Zhang, H.; Cheng, H. N. In Transition Metals and Organometallics as Catalyst for Olefin Polymerization; Kaminsky, W.; Sinn, H, Eds.; Springer Verlag: Berlin, 1988.
27. Chien, J. C. W.; Wang, B. P. J Polym Sci Part A Polym Chem 1990, 28, 15.
28. Fisher, D.; Mlhaupt, R. J Organomet Chem 1991, 417, C7.